# Random Field Ising Model In and Out of Equilibrium

Yang Liu and Karin A. Dahmen
*Department of Physics, University of Illinois at Urbana-Champaign, Urbana, IL 61801, USA*
(Dated: February 6, 2008)

We present numerical studies of zero-temperature Gaussian random-field Ising model (zt-GRFIM) in both equilibrium and non-equilibrium. We compare the no-passing rule, mean-field exponents and universal quantities in 3D (avalanche critical exponents, fractal dimensions, scaling functions and anisotropy measures) for the equilibrium and non-equilibrium disorder-induced phase transitions. We show compelling evidence that the two transitions belong to the same universality class.

PACS numbers: 02.60.Pn, 75.10.Nr, 75.60.Ej, 64.60.Fr

As a prototypical model for magnets with quenched disorder, the random-field Ising Model (RFIM) has been intensively studied during the last thirty years [1]. Nevertheless, some theoretically and experimentally important questions are still not well answered. For example, it is still controversial whether the equilibrium and non-equilibrium disorder-induced phase transitions of the zero-temperature RFIM belong to the same universality class.

The RFIM is defined by the Hamiltonian

$$\mathcal{H} = -\sum_{<i,j>} J\, s_i s_j - \sum_i (H + h_i)\, s_i \qquad (1)$$

where the spins $s_i = \pm 1$ sit on a $D$-dimensional hypercubic lattice with periodic boundary conditions. The spins interact ferromagnetically with their nearest neighbors with strength $J$ and experience a uniform external field $H$ and a local field $h_i$. To model quenched disorders, the local fields $h_i$ are randomly chosen from a Gaussian distribution with mean zero and variance $R$. $R$ is often called the disorder parameter or just disorder.

In equilibrium, it is well known that for $D \geq 3$ there is a continuous phase transition between the ferromagnetic and paramagnetic phases at finite temperatures and disorders [1]. Critical behavior of this transition is controlled by a stable zero-temperature fixed point [2, 3]. Therefore, we can stay at $T = 0$ and study the phase transition undergone by the ground state (GS) as $R$ is tuned to the critical value $R_c$, i.e. the disorder-induced phase transition (DIPT), to obtain the equilibrium properties at finite temperatures [4]. As for the GS problem of the RFIM, it can be mapped onto the min-cut/max-flow problem in combinatorial optimization and then solved via the so-called push-relabel algorithm [5]. In non-equilibrium, the DIPT was first numerically observed by Sethna *et al.* in the hysteretic behavior at $T = 0$ and $D \geq 3$ [6]. A local metastable dynamics was introduced there: As $H$ is slowly increased from $-\infty$ to $\infty$ and decreased back to $-\infty$, each spin flips deterministically when its effective local field $h_i^{\text{eff}} = J\sum_j s_j + h_i + H$ changes sign. It is found that there is a critical point ($R_c$, $H_c$) which separates macroscopically smooth saturation hysteresis loops in the magnetization $M(H)$ (for $R > R_c$) from saturation loops with a macroscopic jump or burst (for $R < R_c$). Here, $H_c$ is the non-universal magnetic field value at which the magnetization curve has infinite slope. (Of course, in equilibrium $H_c = 0$ due to symmetry.) This non-equilibrium DIPT has also been studied analytically [7] and experimentally [8].

Comparing the equilibrium and non-equilibrium DIPTs is very interesting. In mean field theory (MFT), they have the same thermodynamic critical exponents and the same exponent relations [6, 9]. Renormalization group (RG) calculation shows that the $6-\epsilon$ expansion for the non-equilibrium critical exponents maps to all orders in $\epsilon$ onto the equilibrium ones [7], though the RG description of the equilibrium RFIM has been controversial for decades [10]. In 3D and even 4D, numerical values of the critical exponents of the two DIPTs seem to match within the error bars [11, 12, 13].

Recently, Vives *et al.* suggested that the two DIPTs belong to the same universality class by conjecturing the extrapolation result of a RG type argument [14]. Meanwhile, Colaiori *et al.* numerically compared the equilibrium DIPT, i.e. the DIPT of the GS, to that of the demagnetized state (DS), considering the DS as a non-equilibrium hysteretic counterpart of the GS often used in experiments and applications [15]. Here, the DS is obtained by applying an external oscillating field with slowly decreasing amplitude to the non-equilibrium system. The system will then be taken through a series of subloops and the line connecting the tips of those subloops is known as the demagnetization curve. Colaiori *et al.* compare the scaling behavior of the magnetization $M$ for the DS and the GS near their respective $R_c$ and at $H_c$. ($H_c = 0$ for both cases.) Doing finite-size scaling with the known thermodynamic critical exponents, they present evidence that the DIPT of the DS and that of the GS are in the same universality class, in both 3D and the Bethe lattice. On the other hand, Carpenter *et al.* found a related DIPT for the demagnetization curve, which displays similar critical behavior as that of the saturation loop [16].

Despite those evidences in favor of universality, the original question is still not fully answered. We notice that some important critical exponents and universal

quantities of the DIPT of the GS and of the saturation loop have never been compared. Also, we notice that by comparing universal scaling functions rather than just critical exponents, we are comparing an infinite amount of more information than was done previously. (1) *We compare the avalanche exponents and scaling functions associated with the avalanche size distribution.* Here, "avalanche" refers to the flip of neighboring spins during the magnetization process, corresponding to a jump in the magnetization curve $M(H)$. The number of spins participating in an avalanche is called its size $S$. Since in non-equilibrium the avalanche exponents and the associated scaling function have been well studied, comparing them with the corresponding equilibrium ones constitutes a particularly strong test for universality. (2) *We compare the spatial structure of avalanches and clusters near the critical disorder.* Here, clusters are connected regions of flipped spins, formed by the aggregation of avalanches. In non-equilibrium, it is known that near the critical disorder the spatial structure of avalanches is visually interesting: fractal and anisotropic [17]. In equilibrium it also has been found that near the critical disorder clusters have fractal surfaces [18]. Up to now, the comparison of spatial structures of avalanches (or clusters) in equilibrium and non-equilibrium has never been done. This would be another independent test of the universality. We think the whole idea of looking at avalanches and clusters is quite neat: Not only are we directly testing more sensitive features of the problem, but we are giving insight into why the two DIPTs could be similar: the equilibrium and non-equilibrium systems could have similar avalanches and clusters during the magnetization process.

In equilibrium, the magnetization process can be simulated with the efficient algorithm reported in Ref. 19, 20. This algorithm is essentially based on the fact that the GS energy has a convexity property which allows for estimates of the fields where the magnetization jumps (called "avalanches" occur). In non-equilibrium, three different algorithms to simulate the magnetization process (hysteresis loops) are described in Ref. 21. All these algorithms use the adiabatic single-spin-flip dynamics introduced in Ref. 6. In this work, we have studied the magnetization processes in both equilibrium and non-equilibrium for system sizes ranging from $L^3 = 32^3$ to $192^3$. All the measured properties are averaged over a large number of realizations of the random-field configuration. Typical averages are performed over a number of realizations that ranges between $10^4$ for $L = 32$ and 50 for $L = 192$.

Before we present any numerical results in 3D, we show two additional similarities beyond the 3D simulation. (1) *The avalanche critical exponents in MFT must be the same for the two DIPTs.* We start the proof by noticing that in non-equilibrium the hard spin MFT magnetization curve has no hysteresis for $R \geq R_\mathrm{c}$ [7]. Since there is only one $M(H)$ solution for $R \geq R_\mathrm{c}$ in MFT, it must be the non-equilibrium and the equilibrium solution at the same time. In MFT, every spin couples to $M(H)$. Since $M(H)$ is unique, this implies that as $H$ is increased there is a unique series of local-field configurations and therefore a unique series of states. This means that in MFT for $R \geq R_\mathrm{c}$ the avalanches in equilibrium must be the same as the avalanches in non-equilibrium. So the MFT avalanche exponents must be the same in both DIPTs. (2) *Middleton's no-passing rule* [22]: One defines the natural partial ordering of two states: a state $C = \{s_1, \cdots, s_N\} \geq \tilde{C} = \{\tilde{s}_1, \cdots, \tilde{s}_N\}$ if $s_i \geq \tilde{s}_i$ for each site $i$ of the system. Let a system $C(t)$ be evolved under the fields $H(t)$ and similarly $\tilde{C}(t)$ evolved under $\tilde{H}(t)$. Suppose the fields $H(t) \geq \tilde{H}(t)$ and the initial states satisfy $C(0) \geq \tilde{C}(0)$, then the no-passing rule guarantees the partial ordering will be preserved, i.e. $C(t) \geq \tilde{C}(t)$ at all times later $t > 0$. For the magnetization process, this is equivalent to the absence of reverse spin flips as $H$ is swept from $-\infty$ to $\infty$. In non-equilibrium, this rule has been proven and applied to explain the return-point memory [6]. In equilibrium, the main idea of the proof follows. For any state $C_2$ at field $H_2$ which evolves from the GS $C_1$ at field $H_1$ ($H_1 < H_2$) with reverse avalanches, we can always find a corresponding state $\tilde{C}$ which evolves from $C_1$ without any reverse avalanches and has lower energy than $C_2$ at field $H_2$. So as $H$ is increased, the GS evolves without any reverse spin flips. Since flipped spins need not be considered any more in the GS calculation for all higher fields, the algorithm will be accelerated dramatically [20]. For details, see Ref. 23.

Now, we report new 3D simulation results which present evidence of universality for the two DIPTs. First, we extract the avalanche exponents from the field integrated avalanche size distribution $D_\mathrm{int}(S, R)$ associated with the equilibrium magnetization curve, see Fig. 1. In both equilibrium and non-equilibrium, the scaling form of $D_\mathrm{int}(S, R)$ can be written as

$$D_\mathrm{int}(S, R) \sim S^{-(\tau+\sigma\beta\delta)}\ \bar{\mathcal{D}}^\mathrm{int}_{\pm}(S^\sigma |r|) \tag{2}$$

with $r = (R_\mathrm{c} - R)/R$. Note that $R_\mathrm{c}$ is non-universal. For Gaussian disorders in 3D, $R_\mathrm{c}^\mathrm{eq} = 2.270 \pm 0.004$ [18] and $R_\mathrm{c}^\mathrm{neq} = 2.16 \pm 0.03$ [12]. In non-equilibrium, the quantity $D_\mathrm{int}(S, R)$ has been studied extensively, where $(\tau + \sigma\beta\delta)^\mathrm{neq} = 2.03 \pm 0.03$ and $\sigma^\mathrm{neq} = 0.24 \pm 0.02$ were obtained from scaling collapses and linear extrapolation to $R_\mathrm{c}$ [6, 12]. In equilibrium, using the same method, we have $(\tau + \sigma\beta\delta)^\mathrm{eq} = 2.00 \pm 0.01$ and $\sigma^\mathrm{eq} = 0.23 \pm 0.01$. Both $\sigma^\mathrm{eq}$ and $(\tau + \sigma\beta\delta)^\mathrm{eq}$ match their non-equilibrium values. Plotting the non-equilibrium universal scaling function [12]: $\bar{\mathcal{D}}^\mathrm{int}_{-}(X) = e^{-0.789X^{1/\sigma}}(0.021 + 0.002X + 0.531X^2 - 0.266X^3 + 0.261X^4)$ on top of the equilibrium collapse, we find an excellent match, up to the overall horizontal and vertical scaling factors, see inset of Fig. 1. According to this scaling function, we plot the distribution curves on top of the original data, we find excellent

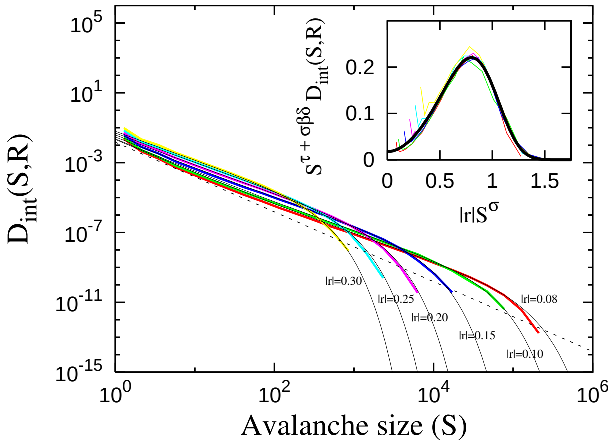


FIG. 1: (Color online) Integrated equilibrium avalanche size distribution curves in 3D for $64^3$ spins and different disorders. Those curves are averaged up to 500 initial random-field configurations. The inset shows the scaling collapse of the integrated avalanche size distribution, using $(\tau+\sigma\beta\delta)^{\rm eq}=2.00$ and $\sigma^{\rm eq}=0.23$. (Even with $(\tau+\sigma\beta\delta)^{\rm neq}=2.03$ and $\sigma^{\rm neq}=0.24$, the collapse still looks good.) The thick black curve through the collapse is the non-equilibrium universal scaling function $\bar{\mathcal{D}}_{-}^{\rm int}(X)$ (see text). In the main panel, the equilibrium distribution curves obtained from the non-equilibrium scaling function are plotted (thin solid lines) alongside the raw data (thick solid lines). The straight dashed line is the expected asymptotic power-law behavior: $S^{-2.00}$, which does not agree with the measured slope of the raw data quoted in Ref. 24 due to the "bump" in the scaling function.

fits for all disorders. The match in both critical exponents and scaling functions strongly indicate that the two DIPTs belong to the same universality class.

Second, we consider the spatial structure of avalanches and clusters at $R_{\rm c}$ in both equilibrium and non-equilibrium. Avalanches are integrated over the field $H$ while clusters are chosen from states near the critical field $H_{\rm c}$. ($H_{\rm c}^{\rm eq}=0$ and $H_{\rm c}^{\rm neq}=1.435\pm0.004$ at $R=R_{\rm c}$ for Gaussian disorder in 3D [12].) The spatial structure can be quantitatively described by fractal dimensions and anisotropy measures. We first compute the fractal dimensions $d_{\rm f}$ of the size (or mass) $S$, enclosed volume $v$ and outermost surface $a$ of avalanches and clusters. Note that the difference between $v$ and $S$ is due to possible "holes" inside avalanches (or clusters) [18]. For finite systems, the natural finite-size scaling hypothesis reads $f(l;R,L)=L^{d_{\rm f}}\hat{f}(rL^{1/\nu},l/L)$. Here, $f$ could be $S$, $v$ or $a$ of the avalanche (or cluster) with linear size $l$ in a system of linear size $L$. $\nu$ is the critical exponent of the correlation length $\xi$ and $\hat{f}$ is a universal scaling function. This hypothesis enables us to do the scaling collapse at $R_{\rm c}$ for different system sizes. Extrapolation values ($L\to\infty$) are quoted in Table I. Here, the error bars include both statistical and systematic errors. We find that $d_{\rm S}=d_{\rm v}$ for all the cases, which indicates the "holes"

TABLE I: Fractal dimensions and anisotropy measures obtained from numerical simulations in 3D for both equilibrium and non-equilibrium zt-GRFIM.

| | non-equilibrium | | equilibrium | |
|---|---|---|---|---|
| Quantities | Avalanches | Clusters | Avalanches | Clusters |
| $d_{\rm S}$ | $2.78\pm0.05$ | $2.76\pm0.04$ | $2.77\pm0.09$ | $2.78\pm0.05$ |
| $d_{\rm v}$ | $2.78\pm0.05$ | $2.76\pm0.04$ | $2.77\pm0.09$ | $2.78\pm0.05$ |
| $d_{\rm a}$ | $2.33\pm0.04$ | $2.18\pm0.04$ | $2.16\pm0.05$ | $2.11\pm0.03$ |
| $A_1$ | $0.29\pm0.01$ | $0.25\pm0.01$ | $0.30\pm0.02$ | $0.28\pm0.01$ |
| $A_2$ | $0.50\pm0.02$ | $0.45\pm0.02$ | $0.50\pm0.02$ | $0.48\pm0.02$ |
| $\Delta_D$ | $0.16\pm0.01$ | $0.21\pm0.02$ | $0.16\pm0.02$ | $0.18\pm0.02$ |
| $S_D$ | $0.06\pm0.01$ | $0.09\pm0.01$ | $0.06\pm0.01$ | $0.07\pm0.01$ |

would be ignorable in the thermodynamic limit. Moreover, considering the systematic errors could be even larger than the ones listed here, we conclude that the fractal dimensions ($d_{\rm S}$, $d_{\rm v}$ or $d_{\rm a}$) of avalanches (or clusters) in equilibrium and non-equilibrium are very close. For the anisotropy measures, as done in the percolation and polymer systems [25], we use the radius of gyration tensor $Q$: $Q_{\alpha\beta}=\frac{1}{2S^2}\sum_{i,j=1}^{S}[X_{i,\alpha}-X_{j,\alpha}][X_{i,\beta}-X_{j,\beta}]$ to characterize the shape of a given conformation of $S$ points in a $D$-dimensional hypercubic lattice, i.e. an avalanche or a cluster of size $S$. Here $X_{i,\alpha}$ is the $\alpha$-coordinate of the $i$-th point with $\alpha=1,...,D$. All the anisotropy measures are related to $Q$'s $D$ eigenvalues: $\lambda_\alpha$ with $\lambda_1\geq\lambda_2\geq\cdots\geq\lambda_D$ and $\bar{\lambda}=(\sum_\alpha\lambda_\alpha)/D$. (1) *Anisotropy* $A_1\equiv\lambda_D/\lambda_1$ and $A_2\equiv\lambda_{\rm D-1}/\lambda_1$, which are the simplest anisotropy measures in 3D. (2) *Asphericity* $\Delta_D=\frac{1}{D(D-1)}\sum_{\alpha=1}^{D}\frac{(\lambda_\alpha-\bar{\lambda})^2}{\bar{\lambda}^2}$, which characterizes the shape's overall deviation from spherical symmetry. (3) *Prolateness* $S_D\equiv(\lambda_1-\bar{\lambda})(\lambda_2-\bar{\lambda})(\lambda_3-\bar{\lambda})/(2\bar{\lambda}^3)$, which distinguishes prolate (positive $S_D$) from oblate shapes (negative $S_D$) in 3D. Asymptotic values of those anisotropy measures in the large size limit can be obtained from the largest avalanches (or clusters) that are not affected by finite-size effects. Results are shown in Table I. It is interesting to mention that avalanches (or clusters) are prolate in both equilibrium and non-equilibrium. More importantly, we find that the asymptotic values of all the anisotropy measures of avalanches (or clusters) in equilibrium and non-equilibrium are very close.

Third, we measure the field integrated avalanche surface area distribution for given sizes at $R_{\rm c}$ in both equilibrium and non-equilibrium. Analogous to the avalanche time distribution obtained in the non-equilibrium study [12], the scaling form of surface area distribution can be written as:

$$D_{\rm a}^{\rm (int)}(S,a)\sim a^{-(\tau+\sigma\beta\delta+\tilde{d}_{\rm a})/\tilde{d}_{\rm a}}\ \mathcal{D}_{\rm a}^{\rm (int)}(a/S^{\tilde{d}_{\rm a}}) \quad (3)$$

with $\tilde{d}_{\rm a}\equiv d_{\rm a}/d_{\rm S}$. Fig. 2 shows the surface area distributions for different avalanche sizes and collapses of those curves using Eq. 3. Here, we use $\tilde{d}_{\rm a}=0.81$ and

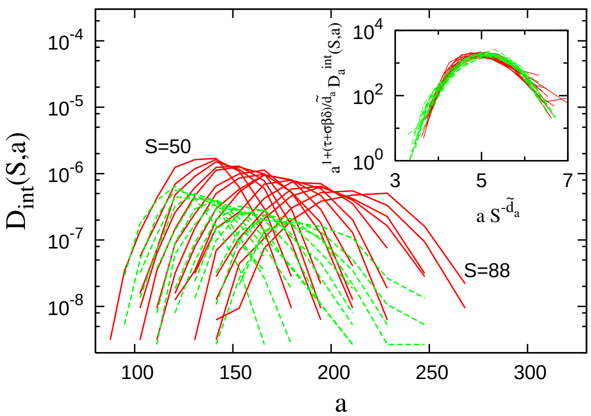


FIG. 2: (Color online) Avalanche surface area distribution curves in 3D at $R_c$, for avalanche size bins from 50 to 88 (from upper left to lower right corner). The system size is $192^3$ for non-equilibrium (solid lines, averaged over 45 initial random-field configurations) and $64^3$ in equilibrium (dashed lines, averaged over 1431 initial random-field configurations). The inset shows the scaling collapse of curves in the main panel, using the same set of exponents for both equilibrium and non-equilibrium: $\tilde{d_a} = 0.81$, $\tau + \sigma\beta\delta = 2.01$.

$\tau + \sigma\beta\delta = 2.01$ for both equilibrium and non-equilibrium collapses. The values are also consistent with what we obtained from the study of the field integrated avalanche size distribution and the fractal dimensions of avalanches. We find that with the same set of exponents, the scaling function $\mathcal{D}_a^{(int)}(X)$ in equilibrium and non-equilibrium match very well.

In summary, we have shown that the equilibrium and non-equilibrium DIPTs of the zt-GRFIM behave surprisingly similarly in critical exponents, scaling functions and spatial structures of avalanches and clusters. Also, they both obey the no-passing rule. All of these results indicate that the two DIPTs are very likely in the same universality class. Larger system sizes could be a direct way to test it further, especially for the fractal dimensions and anisotropy measures. Different disorder distributions and lattice types would also be useful methods to test the universality. Also, we want to emphasize the connection between all the known DIPTs associated with different dynamics (history dependence). As we know, the demagnetization curve displays a very similar DIPT as that of the saturation loop and the ground state [15, 16]. Together with our new result, we suggests that all the three DIPTs, associated with the saturation loop, the demagnetization curve and the equilibrium magnetization curve respectively, are indeed in the same universality class. This would be very exciting. So far there is no RG treatment for the demagnetization curve, while there is for the saturation loop [7]. Motivated by these results, we find that analytic studies comparing the RG descriptions of the DIPTs with different dynamics are indeed an exciting prospect.

We thank James P. Sethna, Andrew Dolgert, A. Alan Middleton, Y. Oono, J. Carpenter, R. White, M. Delgado, and G. Poore for valuable discussions. We acknowledge the support of NSF Grant No. DMR 03-14279 and NSF Grant No. DMR 03-25939 ITR (Materials Computation Center). This work was conducted on the Beowolf cluster of the Materials Computation Center at UIUC.


[1] D. P. Belanger and T. Nattermann, in *Spin Glasses and Random Fields*, edited by A. P. Young (World Scientific, Singapore, 1998).
[2] J. Villain, Phys. Rev. Lett. **52**, 1543 (1984).
[3] D. S. Fisher, Phys. Rev. Lett. **56**, 416 (1986).
[4] A. T. Ogielski, Phys. Rev. Lett. **57**, 1251 (1986).
[5] B. Cherkassky and A. V. Goldberg, Algorithmica **19**, 390 (1997).
[6] J. P. Sethna, K. A. Dahmen, S. Kartha, J. A. Krumhansl, B. W. Roberts, and J. D. Shore, Phys. Rev. Lett. **70**, 3347 (1993).
[7] K. A. Dahmen and J. P. Sethna, Phys. Rev. B **53**, 14872 (1996).
[8] A. Berger, A. Inomata, J. S. Jiang, J. E. Pearson, and S. D. Bader, Phys. Rev. Lett. **85**, 4176 (2000).
[9] T. Schneider and E. Pytte, Phys. Rev. B **15**, 1519 (1977).
[10] D. E. Feldman, Phys. Rev. Lett. **88**, 177202 (2002), and references therein.
[11] A. Maritan, M. Cieplak, M. R. Swift, and J. R. Banavar, Phys. Rev. Lett. **72**, 946 (1994).
[12] O. Perković, K. A. Dahmen, and J. P. Sethna, Phys. Rev. B **59**, 6106 (1999).
[13] A. K. Hartmann, Phys. Rev. B **65**, 174427 (2002).
[14] F. J. Pérez-Reche and E. Vives, Phys. Rev. B **70**, 214422 (2004).
[15] F. Colaiori, M. J. Alava, G. Durin, A. Magni, and S. Zapperi, Phys. Rev. Lett. **92**, 257203 (2004).
[16] J. H. Carpenter and K. A. Dahmen, Phys. Rev. B **67**, 020412 (2003).
[17] J. P. Sethna, K. A. Dahmen, and C. R. Myers, Nature **410**, 242 (2001).
[18] A. A. Middleton and D. S. Fisher, Phys. Rev. B **65**, 134411 (2002).
[19] A. K. Hartmann, PHYSICA A **248**, 1 (1998).
[20] C. Frontera, J. Goicoechea, J. Ortín, and E. Vives, J. Comp. Phys. **160**, 117 (2000).
[21] M. C. Kuntz, O. Perković, K. A. Dahmen, B. W. Roberts, and J. P. Sethna, Comp. Sci. Eng. **1**, 73 (1999).
[22] A. A. Middleton, Phys. Rev. Lett. **68**, 670 (1992).
[23] Y. Liu and K. A. Dahmen, to be published (2006).
[24] C. Frontera and E. Vives, Comp. Phys. Comm. **147**, 455 (2002).
[25] O. Jagodzinski, E. Eisenriegler, and K. Kremer, J. Phys. I France **2**, 2243 (1992).